EGU2010-11628

Climatology of GPS scintillations over Antarctica under solar minimum conditions

L. Spogli[1], L. Alfonsi[1], G. De Franceschi[1], V. Romano[1], C. Mitchell[2]
[1]Istituto Nazionale di Geofisica e Vulcanologia (INGV), Via di Vigna Murata 605, 00143 Rome, Italy
[2]Department of Electronic and Electrical Engineering, University of Bath, Claverton Down, Bath BA2 7AY, United Kingdom
luca.spogli@ingv.it

INTRODUCTION

Ionospheric amplitude and phase scintillations data recorded in Antarctica are analyzed to produce a scintillation climatology over a large geomagnetic quiet period. Within this scope we realize maps of scintillation occurrence as a function of the magnetic local time (MLT) and of the altitude adjusted corrected geomagnetic coordinates (AACGM). Maps of the rate of change of the Total Electron Content (ROT) are also realized to be compared with scintillation occurrence. All the maps are realized merging observations of two GISTMs (GPS Ionospheric Scintillation and TEC Monitor) located at Mario Zucchelli Station (BTN0S - 74.7°S, 164.1°E) and Concordia Station (DMC0S - 75.1°S, 123.2°E) in Antarctica during 2008. The investigation of such phenomena during the solar minimum is important as background for the next solar maximum, expected in 2013, but also for a deeper understanding of the dynamics of the quiet ionosphere. This study, obtained by statistically analysing a large data sample (~7.5 millions of scintillation data), would like also to be a step forward through the development of ionospheric scintillation forecasting algorithms to improve the mitigation of Space Weather (SW) phenomena jeopardizing trans-ionospheric signals.

DATA AND BACKGROUND

Data comes from two GISTMs (GPS Ionospheric Scintillation and TEC Monitor), which consist of NovAtel OEM4 dual-frequency receivers with special firmware specifically able to compute in near real time the amplitude and the phase scintillation from the GPS L1 frequency signals. The amplitude scintillation is monitored by computing the S_4 index, which is the standard deviation of the received power normalized by its mean value. Phase scintillation computation is accomplished by monitoring the σ_ϕ index, the standard deviation of the detrended carrier phase. These indices are both based on 50 Hz measurements at L1 frequency. GISTM's are also able to calculate the ionospheric not-calibrated Total Electron Content and its rate of change (ROT) from both L1 and L2 frequency over time intervals of 15 seconds. Figure 1 shows the location of the receiver sites, Table 1 summarizes the ID, the location, the geographic and corrected geomagnetic coordinates of the GISTM receivers. Concordia Station is located deep in the polar cap through the whole day. Also Mario Zucchelli Station is generally located in the polar cap, however around local noon it approaches the cusp and eventually under the footprint of the closed field lines. The available data along the year 2008 and the corresponding percentage are also indicated, showing a good coverage of the investigated period.

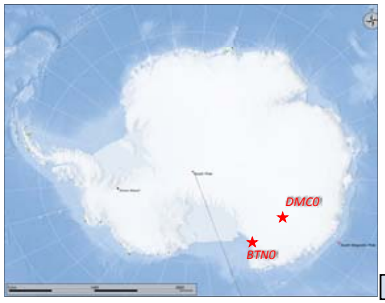

Figure 1. Location of the stations used in the analysis.

ID	Site	Lat	Long	CGLat	CGLon	Days of data	%
DMC0	Concordia Station	75.1°S	123.4°E	88.9°S	54.4°E	319	87.2
BTN0	Mario Zucchelli Station	74.7°S	164.1°E	80.0°S	306.7°E	333	91.0

Table 1. Receiver ID, location sites, geographic and corrected geomagnetic coordinates of the GISTM receivers. The days of available data for the year 2008 and the corresponding percentage are also indicated.

METHOD

We first construct maps of percentage of occurrence of both the scintillation indices evaluated at 60 s in AACGM: Magnetic Latitude (M_{lat}) vs. Magnetic Local Time (MLT). The percentage of occurrence is evaluated for each bin of 1h MLT×1° M_{lat}. To reduce the non-scintillation related tracking errors (such as multipath) only indices computed from observations at elevation angles greater than 20° are considered. Scintillation indices are projected to the vertical, in order to account for varying geometrical effects on the measurements made at different elevation angles. The percentage of occurrence is defined as N_{thr}/N_{tot}, where N_{thr} is the number of data points corresponding to a scintillation index above a given threshold (0.25 radians for σ_ϕ and 0.25 for $S_{4)}$ and N_{tot} is the total number of data points in the bin. Bin with poor statistics (i.e. statistical accuracy > 2.5%) are not considered in the maps. We also produced maps of 1 minute ROT and its root mean square (ROT rms), having the same segmentation of the maps of scintillation occurrence. The method to produce the two maps is the following: starting from the total distribution of the 1 minute values of ROT shown in Figure 2, we extract sub-distributions referring to a given bin. This is done bin by bin and from each of these sub-distribution (one of which is shown, as an example if Figure 3) we extract the mean value and the rms to fill the ROT and ROT rms maps. The maps help in the identification of the regions of the ionosphere in which the gradients of electron density are more intense. All the maps are shown as contour plot.

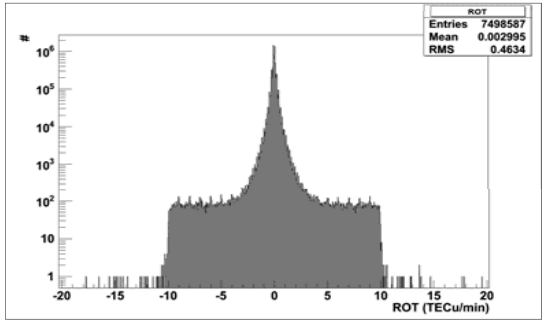

Figure 2. Distribution of ROT of the two receiver for the whole period.

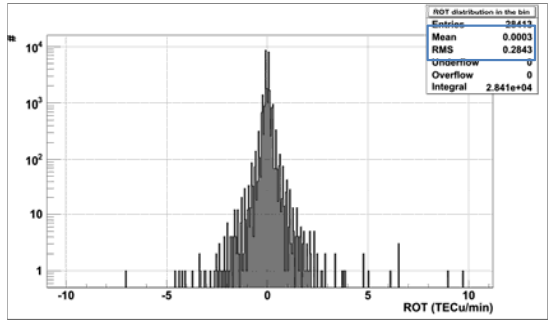

Figure 3. Example of sub-distribution of ROT in a bin

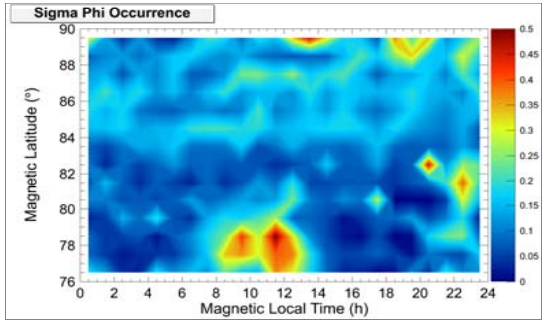

Figure 4. Map of percentage of occurrence of phase scintillation index σ_ϕ.

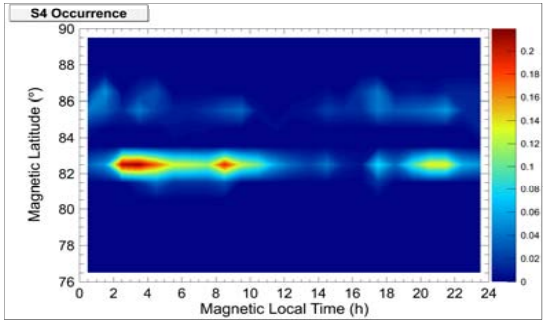

Figure 5. Map of percentage of occurrence of amplitude scintillation index S_4.

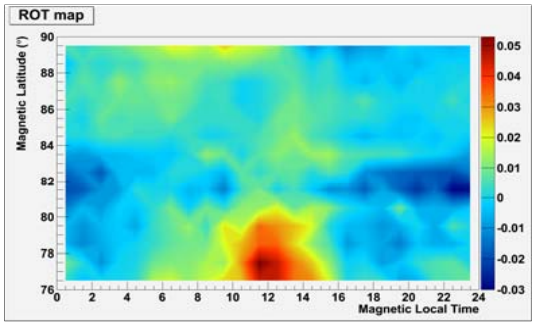

Figure 6. Map of the mean values of the distribution of ROT.

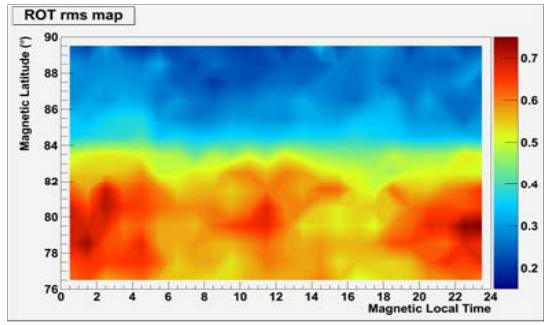

Figure 7. Map of the rms of the ROT distribution.

REMARKS

Figure 4 and Figure 5 show the maps of percentage of occurrence of both indices. The two figures highlight the different behavior of the signal phase scintillation with respect to the amplitude scintillation (scales are different!). Figure 6 shows the map of the mean values of the distribution of ROT and Figure 7 the on of ROT rms. The comparison between Figure 4 and 6 shows that the enhancement of phase scintillation occurrence is co-located with the larger absolute values of ROT, corresponding to the poleward boundary of the auroral oval and to the polar cap patches (mainly in the pre-midnight sector) accordingly with precedent studies (see, e.g., Spogli et al, Ann. Geophys, 2009). The map of ROT rms identifies two main areas, which border appears to be co-located in correspondence of the enhancement of amplitude scintillation occurrence in Figure 5. This correspondence will be further investigated also on the base of a larger statistics covering other phases of the solar cycles.

ACKNOWLEDGEMENTS
The authors would like to thank Andrzej W. Wernik for his kind support and important comments. The authors also thank the Programma Nazionale di Ricerche in Antartide (PNRA), POLRNET-CNR (Consiglio Nazionale delle Ricerche).